Epilepsy Research 151 (2019) 67–74

Contents lists available at ScienceDirect

Epilepsy Research

journal homepage: www.elsevier.com/locate/epilepsyres

Deficiency of urokinase-type plasminogen activator and its receptor affects social behavior and increases seizure susceptibility

Jenni Kyyriäinen[a], Tamuna Bolkvadze[a], Hennariikka Koivisto[b], Anssi Lipponen[a], Laura Oliva Pérez[a], Xavier Ekolle Ndode-Ekane[a], Heikki Tanila[b], Asla Pitkänen[a,*]

[a] Epilepsy Research Laboratory, A. I. Virtanen Institute for Molecular Sciences, University of Eastern Finland, PO Box 1627, FI-70211 Kuopio, Finland
[b] Neurobiology of Memory Laboratory, A. I. Virtanen Institute for Molecular Sciences, University of Eastern Finland, PO Box 1627, FI-70211 Kuopio, Finland

ARTICLE INFO

Keywords:
Behavioral analysis
Double knockout
Pentylenetetrazol
Perineuronal nets
Seizure susceptibility

ABSTRACT

Extracellular proteolysis initiated by the binding of urokinase-type plasminogen activator (uPA) to its receptor (uPAR) regulates the development of inhibitory neuronal circuits in the cerebral cortex and tissue remodeling after epileptogenic brain injury. To study the function of different components of the uPA-uPAR system on behavior and epileptogenesis, and to complement our previous studies on naïve and injured mice deficient in the uPA-encoding gene *Plau* or the uPAR-encoding gene *Plaur*, we analyzed the behavioral phenotype, seizure susceptibility, and perineuronal nets surrounding parvalbumin-positive inhibitory interneurons in *Plau* and *Plaur* (double knockout dKO) mice. In a climbing test, dKO mice showed reduced interest towards the environment as compared with Wt mice ($p < 0.01$). In a social approach test, however, dKO mice spent more time than Wt mice exploring the compartment containing a stranger mouse than the empty compartment ($p < 0.05$). Moreover, in a social interaction test, dKO mice exhibited increased contact time ($p < 0.01$). Compared with Wt mice, the dKO mice also had a longer single contact duration ($p < 0.001$) with the stranger mouse. In the elevated plus-maze, grooming, and marble burying tests, the anxiety level of dKO mice did not differ from that of Wt mice. Rearing time in an exploratory activity test, and spatial learning and memory in the Morris swim navigation task were also comparable between dKO and Wt mice. In the pentylenetetrazol (PTZ) seizure-susceptibility test, dKO mice had a shorter latency to the first epileptiform spike ($p = 0.0001$) and a greater total number of spikes ($p < 0.001$) than Wt mice. The dKO genotype did not affect the number of cortical perineuronal nets. Our findings indicate that *Plau/Plaur*-deficiency leads to a more social phenotype toward other mice with diminished interest in the surrounding environment, and increased seizure susceptibility.

1. Introduction

Urokinase-type plasminogen activator receptor (uPAR) is a glycoprotein linked to the cell membrane by a glycosylphosphatidylinositol anchor (Ploug et al., 1991; Smith and Marshall, 2010). It exerts extracellular proteolytic activity by binding to its ligand, urokinase-type plasminogen activator (uPA) (Ellis et al., 1989; Sato et al., 2002). Because uPAR lacks an intracellular domain, it must interact with adjacent membrane receptors, such as platelet-derived growth factor receptor β, and integrins to initiate intracellular signaling (Eden et al., 2011). uPAR together with its membrane receptors and extracellular ligands, including uPA, vitronectin, and sushi-repeat protein X-linked 2, form the uPAR interactome, which regulates the plasticity of the extracellular matrix during development and after brain injury (Dityatev et al., 2014), as well as cellular proliferation, migration, and invasion (Smith and Marshall, 2010).

PLAUR, a gene encoding uPAR, is a risk gene for autism spectrum disorders (Campbell et al., 2008). *Plaur*-deficient mice develop normally but have a reduced number of parvalbumin-positive (PARV+) interneurons in the cingulate and parietal cortex (Powell et al., 2003; Eagleson et al., 2005). Further, *Plaur*-deficient mice exhibit increased anxiety, impaired social behavior, increased seizure susceptibility, and even spontaneous seizures, depending on the genetic background (Powell et al., 2003; Levitt, 2005; Bae et al., 2010; Bolkvadze et al., 2016). These observations link the *Plaur* gene to autism and genetic epilepsy.

The expression of uPAR and uPA is normally low in neurons, microglia, astrocytes, and vascular cells, but becomes robustly upregulated after epileptogenic brain injury in both experimental models (Lahtinen et al., 2006, 2009) and humans (Liu et al., 2010; Iyer et al.,

* Corresponding author at: Virtanen Institute for Molecular Sciences, University of Eastern Finland, PO FI-70211, Kuopio, Finland.
E-mail address: asla.pitkanen@uef.fi (A. Pitkänen).

https://doi.org/10.1016/j.eplepsyres.2019.02.009
Received 24 October 2018; Received in revised form 1 February 2019; Accepted 23 February 2019
Available online 25 February 2019
0920-1211/

2010). Mice with *Plau* or *Plaur* deficiency have impaired post-injury recovery (Morales et al., 2006; Lahtinen et al., 2010; Ndode-Ekane and Pitkanen, 2013; Rantala et al., 2015; Bolkvadze et al., 2015, 2016). Moreover, the brain tissue of patients with drug-refractory epilepsy exhibits increased uPA and/or uPAR expression (Liu et al., 2010; Iyer et al., 2010). These data show that, in addition to genetically-driven brain disorders, the uPA-uPAR interactome contributes to the post-injury tissue recovery and functional outcome, possibly including acquired epileptogenesis.

We previously characterized the neurophenotype of *Plau*- and *Plaur*-deficient mice and their response to epileptogenic brain injury (Lahtinen et al., 2010; Ndode-Ekane and Pitkanen, 2013; Rantala et al., 2015; Bolkvadze et al., 2015, 2016). To further elucidate the involvement of individual components of the uPAR interactome in normal behavior and the response to stimuli, we performed extensive behavioral testing of double knockout mice (dKO) lacking both *Plau* and *Plaur* in exploratory activity, social interaction, and anxiety, as well as learning and memory tests. To assess the epileptogenicity of the dKO mice, video-encephalography (EEG) monitoring was performed to detect spontaneous seizures and the pentylenetetrazol (PTZ) test was performed to assess seizure susceptibility. Finally, immunohistochemistry using a lectin for *Wisteria Floribunda* was performed on mouse brain tissue to evaluate the cortical perineuronal nets that surround and modify the excitability of PARV + inhibitory interneurons in the cerebral cortex (Wintergerst et al., 1996).

2. Materials and methods

2.1. Animals and genotyping

Adult female and male wild-type (Wt) mice, as well as female and male double knockout (dKO) mice deficient for both the *Plau* and *Plaur* genes were used. All mice were of a C57BL/6 JOlaHsd background. uPA$^{-/-}$ mice [B6.129S2-Plau^{tm1Mlg}/J; the Jackson Laboratory, Bar Harbor, USA (Carmeliet et al., 1994)], lacking exons 3–11, were backcrossed to uPAR$^{-/-}$ mice [B6.129P2-Plaur^{tm1Jld}/J; originally from the Jackson Laboratory (Bugge et al., 1995)], lacking exon 3, for at least eight generations. The genotype was confirmed by polymerase chain reaction analysis of an ear punch sample. Wt and dKO mice used were from the same generation.

To confirm *Plau* deficiency in the dKO mice, we used oIMR0432 (5′ TCTGGAGGACCGCTTATCTG-3′), oIMR0433 (5′CTCTTCTCCAATGTGG GATTG-3′), and oIMR2060 (5′CACGAGACTAGTGAGACGTG-3′) primers (stock number: 002509, Jackson Laboratory). The PCR reaction master mix contained 0.0825 μM oIMR2060, 0.0825 μM oIMR0432, 0.165 μM oIMR0433, and 0.2 mM of each dNTP, 1X DynaZyme reaction buffer containing 1.5 mM $MgCl_2$ and DynaZyme II polymerase (0.03 U/μl, #F-501 L, Thermo Fisher, Waltham, MA, USA). The PCR conditions were as follows: 94 °C for 3 min, 94 °C for 30 s, 60 °C for 1 min, and 72 °C for 1 min using 35 cycles, followed by 72 °C for 2 min. PCR fragments were verified in 1.5 % agarose gels.

To confirm *Plaur* deficiency in the dKO mice, we used *Plaur* primer 1 (5′TATTACCAGTGAATCTTTGTCAGCAGTTCCC-3′), *Plaur* primer 2 (5′ AGAGCTCCGGGTTCTCTCTC-3′), and *Plaur* primer 3 (5′ GGGAGGAA GGAACTCCACTC-3′) (Farris et al., 2011). The PCR reaction master mix contained: 0.0825 μM *Plaur* primer 1, 0.0825 μM *Plaur* primer 3, 0.165 μM *Plaur* primer 2, and 0.2 mM of each dNTP, 1x reaction buffer, 2.0 mM $MgCl_2$, and DreamTaq DNA polymerase (EP0701, Thermo Fisher). The PCR conditions for *Plaur* were as follows: 95 °C for 2 min, 95 °C for 30 s, 64 °C for 30 s, and 72 °C for 30 s using 10 cycles by lowering the annealing temperature 1 °C/cycle, followed by 95 °C for 30 s, 54 °C for 30 s, and 72 °C for 30 s using 40 cycles, and then 72 °C for 5 min. To identify the genotype, PCR fragments were verified in 1.5 % agarose gels.

The mice were housed in a controlled environment (temperature 22 ± 1 °C, humidity 50 %–60 %, light-dark cycle from 07.00 to 19.00) with free access to food and water. All animal procedures were approved by the Animal Ethics Committee of the Provincial Government of Southern Finland, and performed in accordance with the guidelines of the European Community Council Directives 2010/63/EU.

2.2. Behavioral analysis

Behavioral differences between Wt (n = 13; 6 females, 7 males) and dKO (n = 10; 4 females, 6 males) mice were assessed using an extensive battery of behavioral tests of exploratory activity, social interaction, anxiety, and learning and memory. For all the tests, the rater was blind to the mouse genotype.

2.2.1. Exploratory activity

TruScan® (Coulbourn Instruments, Allentown, PA, USA) automated activity monitoring based on detection of breaks of infrared photobeams was used to assess spontaneous locomotion and exploratory activity, as previously described (Rantala et al., 2015). In brief, the system comprises an observation cage with white walls (26 cm × 26 cm × 39 cm) and two rings of photobeam detectors to monitor horizontal and vertical movements. Free exploration was recorded for 10 min. The analyzed parameters included the following: ambulatory distance (gross horizontal locomotion), stereotypy time (time engaged in movements that repeatedly break adjacent beams at least three times), time in the cage center, and vertical time (rearing).

2.2.2. Social approach

Social approach tests measure the exploratory activity and social contact of the animal. The test was performed as previously described by Kaidanovich-Beilin et al. (2011) with minor modifications. The test was performed in a home cage (40 cm × 24 cm × 15 cm) with bedding and two cylindrical cages (height 9 cm, diameter 8 cm, weighted down by a half-filled 60 ml glass beaker on the top) on the opposite ends of the cage. The cylindrical cages were separated by an opaque plastic wall with a mouse-size opening at the bottom of the center of the wall. After a 10-min habituation period, a stranger mouse (same sex as the study mouse) was placed in one of the cylindrical cages. The test was 10-min long and video-recorded. The number of nose contacts with the cylindrical cages and the time spent sniffing were measured from the recording.

2.2.3. Social interaction

The social interaction test was performed as previously described by Sallinen et al. (2013) by adapting the rat protocol to mice. The test was performed in a rectangular arena (79 cm × 57 cm × 20 cm) made of white opaque plastic. The study mouse and a stranger mouse (same sex as the study mouse) were placed on opposite sides of the test arena, and the number and length of contacts between them were monitored and video-recorded for 10 min. The stranger mouse had its back colored white with titanium oxide to allow for identification in the video recording. The test was run twice with a 12-day interval and the stranger mouse was different each time. The number and duration of contacts that the study mouse initiated (sniffing of the rump and other contacts) were calculated off-line from the video separately for the first and last 5-min periods.

2.2.4. Grooming and climbing test

Each mouse was placed individually into a standard mouse cage containing only bedding material. After a 10-min habituation period, the spontaneous behavior of the mouse was video-recorded for 10 min. The time spent grooming and climbing on the lid of the cage were analyzed from the recording.

2.2.5. Elevated plus maze

The elevated plus maze test is a widely used measure of anxiety. The maze comprised four arms (30 cm × 5 cm) radiating from a central

platform (5 cm × 5 cm) 40 cm above the floor. Two of the arms had no walls on any side (Open) and two had a 14-cm high wall on all sides except at the center of the platform (Closed). The maze was made of black plastic, but the arms were covered with white plastic mat to provide contrast with the mouse for the video image. The mouse was placed on the central platform and video-recorded for 5 min. The number of transitions between the arms and the time spent in the open and closed arms were calculated, and the percentage of the total time spent on the open arms was analyzed.

2.2.6. Marble burying test

The marble burying test measures object neophobia. We adopted the version of marble burying test that was shown to be sensitive to the anxiety component in C57Bl/6 J mice (Nicolas et al., 2006). Nine glass marbles (1 cm diameter) were placed overnight in a 3 × 3 array covering half of the cage floor on double the usual amount of fresh bedding. The number of completely covered marbles the next morning was used as an index of anxiety.

2.2.7. Morris swim navigation task

The Morris swim navigation task was used to measure spatial learning and memory. The apparatus was a white plastic wading pool with a diameter of 120 cm A transparent glass platform (14 × 14 cm) was placed 1.0 cm below the water surface. The temperature of the water was maintained at 20 ± 0.5 °C throughout the experiment, and a short recovery period in a warm cage was provided between trials. The mice were first pretrained during two days to find and climb onto the submerged platform by guiding them within a walled alley. In the actual test phase (days 1–4), the mice were given five trials/day with a 10-min rest between trials. On day 5, the platform was removed for the first and last trials to determine the search bias. The platform location was kept constant, but the starting position varied amoung four constant locations at the pool rim, with all mice starting from the same position in any single trial. If the mouse failed to find the escape platform within 60 s, it was placed on the platform for 10 s by the experimenter. The task was video-recorded with a camera mounted on the ceiling. The escape latency and swimming speed were calculated for each trial and then averaged across all 5 days of task acquisition. The search bias during the probe trial was measured by calculating the time the mouse spent within 30 cm from the center of the former platform position.

2.2.8. Passive avoidance

Fear conditioning was tested using the passive avoidance test. The test was performed in a two-compartment light-dark box (42 cm × 32 cm × 22 cm, Med Associates Inc., Fairfax, VA, USA). On the first day, the mouse was allowed to explore the test arena for 5 min. When the mouse entered the dark compartment with all four paws, a sliding door on the dividing wall that contained a mouse-sized hole was closed, and the mouse was confined in the dark compartment for 30 s. The time the mouse took to enter the dark compartment was recorded. The mouse received two mild electric shocks (0.30 mA, 2 s) and was then returned to its home cage. On test day three (48 h later), the mouse was again placed in the lighted side of the two-compartment box. After 30 s, the sliding door was opened and the latency until the mouse entered the dark compartment (all four paws inside) was measured. The mouse was returned to its home cage after entering the dark compartment or when the total test time of 3 min had elapsed.

2.3. Assessment of spontaneous epileptiform activity

2.3.1. Implantation of electrodes

The Wt (n = 13; 6 females, 7 males) and dKO mice (n = 10; 4 females, 6 males) were deeply anesthetized with sodium pentobarbital (60 mg/kg, intraperitoneally [i.p.]) and placed into a stereotaxic frame. A stainless steel screw electrode (E363/96/2.4/SPC Plastics One Inc., Roanoke, VA, USA; 1 mm in diameter) was inserted into the skull bilaterally above the parietal cortex (AP −1.10 mm; ML ± 2.5 mm bregma as a reference point). A reference electrode was inserted into the skull above the right frontal cortex. A ground electrode was inserted into the occipital bone over the cerebellum. All electrodes were connected to a plastic pedestal (MS 363 Plastics One, Inc.), which was cemented onto the skull with dental acrylic. The mice were allowed to recover for at least 1 wk before starting the recordings. The acute surgery-related mortality was 15% (2/13 mice) in Wt and 10% (1/10 mice) in dKO.

2.3.2. Video-EEG monitoring

The 1-week (24/7) video-EEG monitoring was started 1 wk after electrode implantation as previously described by Nissinen et al. (2017) with adaptation of the rat protocol for mice. Briefly, Wt and dKO mice were placed in Plexiglas cages (size 30 × 18 × 21 cm) in which they could move freely (one mouse per cage), and connected to the recording system via a commutator (SL6C, Plastics One Inc, USA). EEG was recorded using the Nicolet One EEG (ver. 5.71) recording system connected to a M40 amplifier (Taugagreining, Iceland) and filtered (high-pass filter cut-off 0.3 Hz, low-pass filter cut-off 100 Hz). The behavior of the mice was recorded using a WV-BP330/GE video camera (Panasonic, wide angle-lens) that was positioned in front of the cages. A wide-angle lens permitted simultaneous videotaping of up to eight mice. EX12LED-3BD-9 W infrared light (Bosch, Canada) was used at night to allow for continuous 24 h/d video monitoring.

2.3.3. Analysis of video-EEG

Digital EEG files were analyzed manually by browsing the entire file on the computer screen. An electroencephalographic seizure was defined as a high-amplitude rhythmic discharge that clearly represented an atypical EEG pattern (repetitive spikes, spike-and-wave discharges, and slow waves) and lasted more than 5 s. An electrographic epileptiform discharge (ED) was defined as rhythmic transients (≥1 s, but < 5 s) containing spikes and uniform sharp-waves.

2.3.4. Assessment of seizure-susceptibility with the pentylenetetrazol (PTZ) test

A PTZ-test was performed after the 1-wk video-EEG monitoring to define the genotype or sex effects on seizure susceptibility. We administered a subconvulsant dose (50 mg/kg, i.p.) of PTZ (1.5-pentamethylenetetrazole, 98%, Sigma-Aldrich YA-Kemia Oy, Finland) that was dissolved in sterile 0.9% saline (Bolkvadze et al., 2012). Each mouse received a single injection of PTZ.

The outcome measures included the latency to the first spike, total number of spikes, latency to the first electrographic seizure, seizure occurrence (% of mice that seized), and mortality (%) for 60 min after PTZ administration. Spikes were defined as high-amplitude (twice the baseline) sharply contoured waveforms lasting 20–70 msec. For statistical analysis of the number of spikes, we included only those animals that survived at least 60 min after the PTZ injection. The total number of spikes did not include the electrographic seizure events.

2.4. Histology

2.4.1. Fixation and processing of samples

For histology, the mice were deeply anesthetized with sodium pentobarbital (60 mg/kg, i.p.) and then transcardially perfused with 0.9 % saline (5 ml/min, 4 °C, for 2 min) followed by 4% paraformaldehyde (PFA) in 0.1 M sodium phosphate buffer (PB), pH 7.4 (5 ml/min, 4 °C, for 20 min). The brains were removed from the skull, post-fixed in 4 % PFA for 4 h (4 °C), cryoprotected (20 % glycerol in 0.02 M potassium phosphate-buffered saline (KPBS), pH 7.4) for 24 h, frozen in dry ice, and stored at −70 °C until sectioning.

Coronal sections were cut (1-in-6 series, 25-μm thick) with a sliding microtome. The first series of sections was stored in 10 % formalin at

Table 1
Neurophenotype of *Plau/Plaur* double knockout mice (dKO).

Behavioral test	Wt (13)	dKO (10)	*p-value*
Exploratory activity ^{*F} center time (s)	116 ± 41	179 ± 63	< 0.01
Exploratory activity stereotypy time (s)	56 ± 21	54 ± 15	n.s.
Exploratory activity rearing time (s)	52 ± 14	50 ± 15	n.s.
Exploratory activity ^{*M} ambulatory distance (cm)	1468 ± 384	1392 ± 245	n.s.
Social approach stranger mouse (s)	353 ± 64	423 ± 60	< 0.05
Social interaction rump sniff time (s)	2 ± 1	5 ± 6	n.s.
Social interaction ^{*F} total contact time (s)	32 ± 12	53 ± 19	< 0.01
Social interaction ^{*M} contact duration (s)	2 ± 0.4	4 ± 1	< 0.001
Grooming (s)	16 ± 13	26 ± 17	n.s.
Climbing (s) ^{*F}	223 ± 58	151 ± 46	< 0.01
Elevated plus maze open arm (s)	38 ± 38	23 ± 10	n.s.
Elevated plus maze closed arm (s)	146 ± 55	166 ± 36	n.s.
Elevated plus maze center (s)	108 ± 50	110 ± 31	n.s.
Marble burying ^{*M} visible marbles	7 ± 2	5 ± 3	n.s.
Morris swim navigation task swim speed (d1-d5, cm/s)	20 ± 1	21 ± 3	n.s.
Morris swim navigation task escape latency (d1-d5, s)	25 ± 7	26 ± 6	n.s.
Morris swim navigation task mean distance to platform center (probe d5, cm)	37 ± 5	36 ± 6	n.s.
Passive avoidance freezing (d2, s)	83 ± 64	75 ± 58	n.s.

Abbreviations: dKO, double knockout (*Plau/Plaur*-deficient); n.s., statistically not significant; s, seconds; Wt, wild-type. Data are shown as mean ± SD. Number of mice is in parentheses. Statistical significances compared with corresponding genotype (two-way ANOVA; Kruskal-Wallis test followed by Mann-Whitney *U* test). * Indicates genotype effect within the same sex (F = in females; M = in males).

room temperature (RT) for thionin staining. The other series of sections were collected in tissue-collecting solution (30 % ethylene glycol, 25 % glycerol in 0.05 M PB) and stored at −20 °C until further processing.

2.4.2. Nissl staining

To assess the cytoarchitectonic areas of different brain areas, the first series of sections was stained with thionin, cleared in xylene, and cover-slipped using Depex® (BDH Chemical, Poole, UK) as a mounting medium.

2.4.3. Immunohistochemistry and stereological analysis of perineuronal nets positive cells

Every other section from the 1-in-6 series (300 µm apart) of both genotypes (Wt: n = 5, 3 females, 2 males; dKO: n = 5 dKO, 1 female, 4 males) was stained for perineuronal nets, a marker of parvalbumin interneurons (Franklin and Paxinos, 2008). Coronal sections between the anteroposterior levels +2.8 and −4.24 relative to bregma (mouse brain atlas of Franklin and Paxinos, 2008) were selected for analysis. Immunohistochemical staining was performed as previously described by Huusko et al. (2015). Sections were washed three times (10 min each) in 0.02 M KPBS and endogenous peroxidase was removed by incubating in 1% H_2O_2 in 0.02 M KPBS at RT for 15 min. After washing six times in 0.02 M KPBS, sections were blocked in 10% normal horse serum (NHS) and 0.5% Triton X-100 (TX-100) in 0.02 M KPBS at RT for 2 h. Thereafter, sections were incubated with a biotin-conjugated lectin from Wisteria Floribunda (1:4000, PV235, Sigma L-1516, Saint Louis, MO, USA). After washing three times in 0.02 M KPBS, the sections were then incubated in avidin-biotin solution for one hour at RT (Vector Laboratories, Burlingame, CA, USA). Subsequently, they were washed three times in 0.02 M KPBS, and the antigen was visualized by incubation for 2 min in 0.1 % 3′,3′-diaminobenzidine (Pierce Chemicals, Rockford, IL) solution containing 0.04 % H_2O_2 and 0.02 M KPBS. The sections were washed one time in 0.02 M KPBS and two times in 0.1 M PB, and mounted on gelatin-coated microscope slides.

2.4.4. Stereological analysis of perineuronal nets positive cells

Immuno-positive perineuronal net-covered cells were counted throughout the entire cortex of the right hemisphere using unbiased stereology. The analysis included every other section from a 1-in-6 series, starting from bregma level +2.8 to −4.24 rosto-caudally (15–18 sections). The cells were counted using the optical fractionator method as previously described (Kyyriainen et al., 2017). A sampling grid of 300 µm (x-axis) by 300 µm (y-axis) and a counting frame of 60 µm (x-axis) by 30 µm (y-axis) was used. The area sampling fraction (asf) was 0.02, the section sampling fraction (ssf) was 12 and the tissue sampling faction (tsf) was 1. The total number of cells was estimated using the formular: $N_{tot} = \Sigma Q \times 1/ssf \times 1/asf \times 1/tsf$, where N_{tot} is the total number and ΣQ is the combined cell number.

2.5. Statistical analysis

Statistical analysis was performed using IBM SPSS Statistics (v.23). The normal distribution of the data was tested with Kolmogorov-Smirnov test. In cases with no normal distribution, we used nonparametric tests. Normally distributed data was analyzed using two-way ANOVA or repeated measure ANOVA. The nonparametric Kruskal–Wallis test was used to analyze differences between groups in behavioral data, followed by *post hoc* analysis with the Mann–Whitney *U* test. Differences in mortality and number of mice developing epileptiform activity during the PTZ-test were assessed with the $\chi 2$-test. Data are presented as mean ± standard deviation (SD). A p value of less than 0.05 was considered statistically significant.

3. Results

3.1. Behavioral testing

To investigate whether the *Plau/Plaur* genetic deficiency affected behavior, Wt and dKO mice were subjected to an extensive battery of behavioral tests aimed at elucidating genotype differences in anxiety, activity, social interactions, and learning and memory. The results are summarized in Table 1.

3.1.1. Anxiety

Anxiety-related behavior was analyzed using the elevated plus maze, marble burying (object neophobia), and self-grooming tests.

Elevated plus maze. We found no genotype effect as the time spent in the open arms did not differ between the Wt and dKO mice ($p > 0.05$; Table 1).

Grooming test. There was no genotype difference in grooming duration between genotypes ($p > 0.05$; Table 1).

Marble burying test. The number of unburied marbles was not different between genotypes ($p > 0.05$; Table 1).

3.1.2. Exploratory activity and climbing

Spontaneous exploratory activity in a new cage was assessed by calculating ambulatory distance (gross horizontal locomotion), time spent performing stereotypic movements, time spent in the cage center, and rearing time.

Ambulatory distance ($p > 0.05$; Table 1) and the time spent performing stereotypic movements did not differ between genotypes ($p > 0.05$). The time spent in the center of the cage was different between genotypes as dKO mice spent more time in the center of the cage than Wt mice (179 ± 63 s vs. 116 ± 41 s, $p < 0.01$; Table 1). Rearing time did not differ between genotypes ($p > 0.05$). In the additional climbing test, dKO mice spent less time climbing than Wt mice (151 ± 46 s vs. 223 ± 58 s, $p < 0.01$; Table 1).

3.1.3. Social behavior

Social behavior was analyzed using social approach and social interaction tests, where the number and duration of contacts with the stranger mouse were calculated.

In the social approach test, we found an overall genotype effect as dKO mice spent more time exploring the stranger mouse in the cage (vs. the empty cage) than Wt mice (423 ± 60 s vs. 353 ± 64 s, $p < 0.05$; Table 1).

In the social interaction test, we found an overall genotype effect as dKO mice had more contact time with the stranger mouse than Wt mice (53 ± 19 s vs. 32 ± 12 s, $p < 0.01$). Furthermore, the average duration of a single contact was longer for dKO than Wt mice (4 ± 1 s vs. 2 ± 0.4 s, $p < 0.001$). Sniffing time was comparable between genotypes ($p > 0.05$).

3.1.4. Learning and memory

Learning and memory were assessed using passive avoidance and Morris swim navigation task.

Passive avoidance. The time to enter the dark compartment after conditioning did not differ between genotypes (Wt 83 ± 64 s vs. dKO 75 ± 58 s, $p > 0.05$; Table 1).

Morris swim navigation task. Supplementary Fig. 1 shows the learning curve (latency to find the platform) for Wt and dKO mice. The average escape latency across the 5 days of task acquisition (Wt 25 ± 7 s vs. dKO 26 ± 6 s) or the average swimming speed revealed no genotype difference (Wt 20 ± 1 cm/s vs. dKO 21 ± 3 cm/s). Also, the probe test on day 5 to measure search bias as the time spent in the vicinity of the former platform location revealed no genotype differences (by quadrants, SE: Wt 23 ± 6 s vs. dKO 23 ± 8 s; SW: Wt 15 ± 6 s vs. dKO 18 ± 10 s; NW: Wt 10 ± 5 s vs. dKO 9 ± 5 s; NE: Wt 11 ± 5 s vs. dKO 10 ± 5 s; all, $p > 0.05$).

3.2. Video-EEG monitoring and seizure susceptibility test

To assess whether *Plau* and *Plaur* double-deficiency predisposes to spontaneous epileptiform events, Wt and dKO mice were monitored with video-EEG prior to the PTZ seizure-susceptibility test. None of the Wt or dKO mice had spontaneous seizures during the 1-wk video-EEG monitoring period. A summary of the results is shown in Table 2.

The mortality related to status epilepticus following PTZ administration was 18 % (2/11 mice) in Wt and 33 % (3/9 mice) in dKO ($p > 0.05$, χ2-test). In the whole group of mice, the total mortality rate (surgery related and after PTZ administration) did not differ between Wt (31 %, 4 of 13) and dKO mice (40 %, 4 of 10; $p > 0.05$, χ2-test).

Latency to the 1st epileptiform spike. We found a genotype effect on the latency to the 1st epileptiform spike, as it was shorter in dKO mice than in Wt mice (96 ± 26 s vs. 217 ± 58 s, $p = 0.0001$).

Number of epileptiform spikes within 60 min after PTZ injection. We found a genotype effect, as dKO mice had a greater number of epileptiform spikes than Wt mice (222 ± 68 vs. 65 ± 26, $p < 0.001$).

Latency to the 1st electrographic seizure. We found a genotype effect, as the latency to the first electrographic seizure after PTZ administration was shorter in dKO mice than in Wt mice (195 ± 37 s vs. 388 ± 175 s, $p < 0.05$).

Other. No genotype effect was observed in the percentage of mice with electrographic seizures, seizure duration, latency to the first epileptiform discharge (ED), or number of EDs ($p > 0.05$) (Table 2).

3.3. Genotype effect on perineuronal nets

To determine whether the increased susceptibility of dKO mice to PTZ-induced seizures was related to the number and/or functionality of

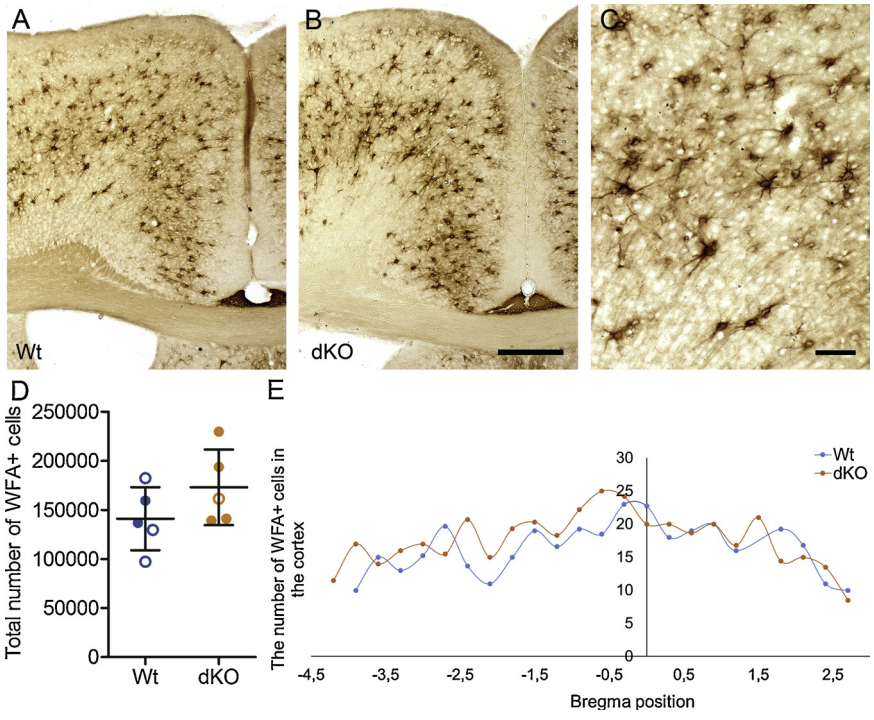

Fig. 1. Lack of genotype effect on the number of perineuronal nets. Lectin from Wisteria Floribunda showing the distribution and density of the perineuronal nets in the cingulate cortex (bregma level 0.14 mm according to the mouse brain atlas of Franklin and Paxinos, 2008 **(A)** in a wild-type (Wt) mouse and **(B)** a *Plau*/Plaur deficient mouse (dKO). **(C)** A high-magnification photomicrograph showing the morphology of perineuronal nets in a Wt mouse. **(D)** Estimation of the total number of perineuronal nets, labelled with lectin for *Wisteria Floribunda* (WFA; y-axis) in the cerebral cortex in Wt (n = 5) and dKO (n = 5) mice (levels AP 2.8 to -4.24, according to the mouse brain atlas of Franklin and Paxinos, 2008). No genotype effect on the total number of perineuronal nets was detected (closed dots – males; open dots – females). **(E)** No genotype effect on the number of perineuronal nets (y-axis) was detected along the rostrocaudal axis (x-axis) of the cerebral cortex in Wt and dKO mice. Data are presented as mean ± SD. Scale bars: 100 µm in panels A and B, 50 µm in panel C.

Table 2
Effect of genotype on the pentylenetetrazol (PTZ) seizure susceptibility test.

Parameter analyzed	Wt	dKO	*p-value*
Latency to the 1st epileptiform spike (s) *F,M	217 ± 58 (10)	96 ± 26 (9)	=0.0001
Latency to the 1st electrographic seizure (s)	388 ± 175 (4)	195 ± 37 (3)	< 0.05
Latency to the 1st electrographic ED (s)	526 ± 482 (2)	123 ± 43 (2)	n.s.
Number of spikes (during 60 min) *F,M	65 ± 26 (9)	222 ± 68 (6)	< 0.001
Number of EDs (during 60 min)	1 ± 0 (2)	1 ± 0 (2)	n.s.
% of mice with PTZ-induced electrographic seizures	36% (4/11)	33% (3/9)	n.s.
Mean duration of induced seizure (s)	19 ± 3 (4)	23 ± 2 (3)	n.s.
PTZ-test related mortality	18% (2/11)	33% (3/9)	n.s.

Abbreviations: dKO, double knockout (*Plau/Plaur*-deficient); ED, epileptiform discharge; n.s., statistically not significant; PTZ, pentylenetetrazol; s, seconds; Wt, wild-type. Data are shown as mean ± SD. Number of mice is in parentheses. Statistical significance compared with corresponding genotype (Mann-Whitney *U* test; χ2-test). * Indicates genotype effect within the same sex (F = within females; M = within males).

PARV + interneurons, we estimated the number of perineuronal nets in the cerebral cortex (Hartig et al., 1992; Wintergerst et al., 1996; Kwok et al., 2011). Perineuronal net immunostaining was used as an indirect method of assessing PARV + interneurons, since perineuronal nets are primarily found around GABAergic positive parvalbumin interneuron (Sorg et al., 2016).

In the whole group of animals, there was no genotype effect on the total number of perineuronal nets (Wt 141,120 ± 32,117 vs. dKO 173,040 ± 38,600, $p > 0.05$; Fig. 1A–D). Also, analysis of the rostro-caudal distribution of perineuronal net-positive cells in the cerebral cortex did not reveal any genotype difference between Wt and dKO mice ($p > 0.05$; Fig. 1E).

4. Discussion

The aim of the present study was to evaluate the neurophenotype of mice deficient for both the *Plau* and Plaur genes. We hypothesized that the phenotype of dKO mice would combine the previously described, somewhat different, phenotypes of *Plau*-deficient mice and *Plaur*-deficient mice.

4.1. dKO mice are more interested in other mice and less interested in the environment than Wt mice, but exhibit no major difference in anxiety, motor activity, or spatial learning and memory

Single nucleotide polymorphisms in the *PLAUR* gene predispose to autism spectrum disorder characterized by deficits in social interaction (Campbell et al., 2008). Accordingly, *Plaur*-deficient animals demonstrate anxiety-like behavior in elevated plus-maze and light-dark avoidance tests (Powell et al., 2003). We have previously reported non-anxious phenotype in *Plau*-deficient mice (Rantala et al., 2015). Similar to Plau-deficiency, dKO phenotype can be interpreted as non-anxious or active.

It has been suggested that due to increased anxiety, *Plaur*-deficient mice show impaired social behavior in social interaction test, spending less time interacting with a stranger mouse compared with Wt mice (Levitt, 2005). Unexpectedly, however, dKO mice were more social than Wt mice in the social approach and social interaction tests. Since no studies of social behavior in *Plau*-deficient animals are available, one can speculate that a double-deficiency (*Plau* and *Plaur*) can result in an erasure of some of the phenotypic features seen in the single KO mice. It remains to be explored whether other mechanisms compensate the lacking ligand and/or receptor function.

We found some indications of reduced interest among dKO mice to explore their environment in the different tests consistent with *Plau*-deficient mice, which we previously reported to be nonchalant towards the environment (Rantala et al., 2015). Our preliminary observations on possible sex differences need to be confirmed in larger animal populations.

The performance of dKO mice in the Morris swim navigation task and the passive avoidance tests was consistent with previous data from Bissonette et al. (2014), who reported unaltered spatial learning in *Plaur*-deficient mice in the Morris swim navigation task. In agreement with previous reports on *Plau* or *Plaur*-deficient mice, dKO mice exhibited no obvious impairment in motor function (Powell et al., 2003; Rantala et al., 2015). We consider it unlikely that the reduced climbing activity of dKO mice relates to impaired motor function because the swimming speed in Morris swim navigation task and rearing time during spontaneous exploration of the new cage did not differ from that of Wt mice.

Taken together, the neurophenotype of dKO mice differed from that of *Plaur*-deficient mice, suggesting that deletion of the expression of the uPAR extracellular ligand uPA contributes to the development of the behavioral phenotype.

4.2. dKO mice show increased susceptibility to PTZ-induced seizures

Previous studies demonstrated that approximately 5 % of *Plaur*-deficient mice exhibit spontaneous seizures (Powell et al., 2003). To date, *Plau*-deficiency has not been associated with the occurrence of spontaneous seizures (Rantala et al., 2015; Bolkvadze et al., 2016). Our 1-wk continuous video-EEG monitoring did not reveal any spontaneous epileptiform activity in dKO mice. As previous studies suggested that the occurrence of epilepsy in *Plaur*-deficient mice may depend on the genetic background (Eagleson et al., 2005; Ndode-Ekane and Pitkanen, 2013; Bolkvadze et al., 2016), it remains to be explored whether the lack of spontaneous seizures in our *Plau/Plaur*-deficient mice also relates to the genetic background.

However, dKO mice had a clearly increased susceptibility to PTZ-induced seizures as both the latency to the first spike and to the 1st electrographic seizure was decreased, and the number of induced seizures during a 60-min follow-up was increased. Our observations are consistent with the data by Powell et al. (2003), who demonstrated a comparable decrease in the latency to seizures, and an increase in seizure severity in *Plaur*-deficient mice. So far, *Plau*-deficiency has not been associated with genetic or acquired seizure susceptibility (Rantala et al., 2015; Bolkvadze et al., 2016).

Taken together, our data indicate that like *Plaur*-deficient mice, dKO mice have increased seizure susceptibility, emphasizing the possible role of uPAR expression in genetic epilepsies.

4.3. Plau/Plaur-deficiency did not affect the number of perineuronal nets in the cerebral cortex

Previous studies demonstrated that uPAR is necessary for the normal development of GABAergic neurons, particularly those expressing PARV (Eagleson et al., 2005). Our data show that the dKO mice exhibited increased seizure susceptibility, which could relate to PARV + interneuronopathy (Price et al., 2009; Katsarou et al., 2017). Several studies have shown that PARV + neurons are surrounded by

perineuronal nets, the integrity of perineuronal nets is a sensitive marker for PARV + neuron function, the perineuronal nets are sensitive to injury, and that the perineuronal nets involved in neuronal and cortical plasticity after stroke and TBI (Hobohm et al., 2005; Kwok et al., 2011; Madinier et al., 2014; Wiley et al., 2016; Hsieh et al., 2017; Hartig et al., 2017; Kim et al., 2017). Therefore, we next assessed the genotype effect on perineuronal nets as a surrogate marker for PARV + neuronal numbers and function. As the loss of PARV-expressing cells in *Plaur*-deficient mice was specifically reported in the cingulate and parietal cortex, rather than more caudally (Powell et al., 2003; Eagleson et al., 2005), we also assessed the rostro-caudal gradient in the number of perineuronal nets.

Our visual or quantitative analyses revealed no genotype effects on perineuronal nets. It remains to be explored whether the inability to demonstrate reduced numbers of perineuronal nets in dKO mice relates to the difference in the genetic background compared with studies in *Plaur*-deficient mice. Interestingly, *Plaur*-deficient mice maintained on a C57BL/6 J/129 Sv background had up to 90 % PARV + neuronal loss (Powell et al., 2003), whereas *Plaur*-deficient mice with a C57BL/6 J background were reported to have a 50 % loss (Eagleson et al., 2005). Another difference between the studies relates to the type of mutation. Our mice were generated by deleting the genomic sequence compromising exon 3 (Bugge et al., 1995), whereas the mice phenotyped by Powell et al. (2003) had deletions of exons 2 through 5 of the *Plaur* gene (Dewerchin et al., 1996). Finally, our data with limited animal number did not suggest even a trend to sex difference in the number of WFA + elements.

5. Conclusion

To our knowledge, this is the first study to evaluate the neurophenotype related to deficient *Plau/Plaur* genotype. Our findings revealed that *Plau/Plaur*-deficiency results in genotype effects, in particular, dKO mice exhibited increased social behavior. Moreover, dKO mice showed a clear increase in seizure susceptibility. Unexpectedly, dKO mice did not exhibit an anxious phenotype in the elevated plus-maze or marble burying tests. These data expand previous observations, and support the role of the uPAR-interactome in behavioral and seizure disorders.

Conflicts of interest

The authors confirm that there are no conflicts of interest.

Acknowledgements

This study was supported by the Academy of Finland, The Instrumentarium Foundation, Epilepsy Foundation, and Maire Taponen Foundation. We thank Mr. Jarmo Hartikainen and Mrs. Merja Lukkari for their excellent technical assistance.

Appendix A. Supplementary data

Supplementary material related to this article can be found, in the online version, at doi:https://doi.org/10.1016/j.eplepsyres.2019.02.009.

References

Bae, M.H., Bissonette, G.B., Mars, W.M., Michalopoulos, G.K., Achim, C.L., Depireux, D.A., Powell, E.M., 2010. Hepatocyte growth factor (HGF) modulates GABAergic inhibition and seizure susceptibility. Exp. Neurol. 221, 129–135.
Bissonette, G.B., Bae, M.H., Suresh, T., Jaffe, D.E., Powell, E.M., 2014. Prefrontal cognitive deficits in mice with altered cerebral cortical GABAergic interneurons. Behav. Brain Res. 259, 143–151.
Bolkvadze, T., Pitkanen, A., 2012. Development of post-traumatic epilepsy after controlled cortical impact and lateral fluid-percussion-induced brain injury in the mouse. J. Neurotrauma 29, 789–812.
Bolkvadze, T., Rantala, J., Puhakka, N., Andrade, P., Pitkanen, A., 2015. Epileptogenesis after traumatic brain injury in Plau-deficient mice. Epilepsy Behav. 51, 19–27.
Bolkvadze, T., Puhakka, N., Pitkanen, A., 2016. Epileptogenesis after traumatic brain injury in Plaur-deficient mice. Epilepsy Behav. 60, 187–196.
Bugge, T.H., Suh, T.T., Flick, M.J., Daugherty, C.C., Romer, J., Solberg, H., Ellis, V., Dano, K., Degen, J.L., 1995. The receptor for urokinase-type plasminogen activator is not essential for mouse development or fertility. J. Biol. Chem. 270, 16886–16894.
Campbell, D.B., Li, C., Sutcliffe, J.S., Persico, A.M., Levitt, P., 2008. Genetic evidence implicating multiple genes in the MET receptor tyrosine kinase pathway in autism spectrum disorder. Autism Res. 1, 159–168.
Carmeliet, P., Schoonjans, L., Kieckens, L., Ream, B., Degen, J., Bronson, R., De Vos, R., van den Oord, J.J., Collen, D., Mulligan, R.C., 1994. Physiological consequences of loss of plasminogen activator gene function in mice. Nature 368, 419–424.
Dewerchin, M., Nuffelen, A.V., Wallays, G., Bouche, A., Moons, L., Carmeliet, P., Mulligan, R.C., Collen, D., 1996. Generation and characterization of urokinase receptor-deficient mice. J. Clin. Invest. 97, 870–878.
Dityatev, A., Wehrle-Haller, B., Pitkanen, A., 2014. Preface. Brain extracellular matrix in health and disease. Prog. Brain Res. 214, xiii–xvii.
Eagleson, K.L., Bonnin, A., Levitt, P., 2005. Region- and age-specific deficits in gamma-aminobutyric acidergic neuron development in the telencephalon of the uPAR(-/-) mouse. J. Comp. Neurol. 489, 449–466.
Eden, G., Archinti, M., Furlan, F., Murphy, R., Degryse, B., 2011. The urokinase receptor interactome. Curr. Pharm. Des. 17, 1874–1889.
Ellis, V., Scully, M.F., Kakkar, V.V., 1989. Plasminogen activation initiated by single-chain urokinase-type plasminogen activator. Potentiation by U937 monocytes. J. Biol. Chem. 264, 2185–2188.
Farris, S.D., Hu, J.H., Krishnan, R., Emery, I., Chu, T., Du, L., Kremen, M., Dichek, H.L., Gold, E., Ramsey, S.A., Dichek, D.A., 2011. Mechanisms of urokinase plasminogen activator (uPA)-mediated atherosclerosis: role of the uPA receptor and S100A8/A9 proteins. J. Biol. Chem. 286, 22665–22677.
Franklin, K.B.J., Paxinos, G., 2008. The Mouse Brain in Stereotaxic Coordinates, 3rd edn. Elsevier Academic, London.
Hartig, W., Brauer, K., Bruckner, G., 1992. Wisteria floribunda agglutinin-labelled nets surround parvalbumin-containing neurons. Neuroreport 3, 869–872.
Hartig, W., Mages, B., Aleithe, S., Nitzsche, B., Altmann, S., Barthel, H., Krueger, M., Michalski, D., 2017. Damaged neocortical perineuronal nets due to experimental focal cerebral ischemia in mice, rats and sheep. Front. Integr. Neurosci. 11, 15.
Hobohm, C., Gunther, A., Grosche, J., Rossner, S., Schneider, D., Bruckner, G., 2005. Decomposition and long-lasting downregulation of extracellular matrix in perineuronal nets induced by focal cerebral ischemia in rats. J. Neurosci. Res. 80, 539–548.
Hsieh, T.H., Lee, H.H.C., Hameed, M.Q., Pascual-Leone, A., Hensch, T.K., Rotenberg, A., 2017. Trajectory of parvalbumin cell impairment and loss of cortical inhibition in traumatic brain injury. Cereb. Cortex 27, 5509–5524.
Huusko, N., Romer, C., Ndode-Ekane, X.E., Lukasiuk, K., Pitkanen, A., 2015. Loss of hippocampal interneurons and epileptogenesis: a comparison of two animal models of acquired epilepsy. Brain Struct. Funct. 220, 153–191.
Iyer, A.M., Zurolo, E., Boer, K., Baayen, J.C., Giangaspero, F., Arcella, A., Di Gennaro, G.C., Esposito, V., Spliet, W.G., van Rijen, P.C., Troost, D., Gorter, J.A., Aronica, E., 2010. Tissue plasminogen activator and urokinase plasminogen activator in human epileptogenic pathologies. Neuroscience 167, 929–945.
Kaidanovich-Beilin, O., Lipina, T., Vukobradovic, I., Roder, J., Woodgett, J.R., 2011. Assessment of social interaction behaviors. J. Vis. Exp.(48). https://doi.org/10.3791/2473. pii: 2473.
Katsarou, A.M., Moshe, S.L., Galanopoulou, A.S., 2017. Interneuronopathies and their role in early life epilepsies and neurodevelopmental disorders. Epilepsia Open 2, 284–306.
Kim, S.Y., Senatorov Jr, V.V., Morrissey, C.S., Lippmann, K., Vazquez, O., Milikovsky, D.Z., Gu, F., Parada, I., Prince, D.A., Becker, A.J., Heinemann, U., Friedman, A., Kaufer, D., 2017. TGFbeta signaling is associated with changes in inflammatory gene expression and perineuronal net degradation around inhibitory neurons following various neurological insults. Sci. Rep. 7 7711-017-07394-3.
Kwok, J.C., Dick, G., Wang, D., Fawcett, J.W., 2011. Extracellular matrix and perineuronal nets in CNS repair. Dev. Neurobiol. 71, 1073–1089.
Kyyriainen, J., Ekolle Ndode-Ekane, X., Pitkanen, A., 2017. Dynamics of PDGFRbeta expression in different cell types after brain injury. Glia 65, 322–341.
Lahtinen, L., Lukasiuk, K., Pitkanen, A., 2006. Increased expression and activity of urokinase-type plasminogen activator during epileptogenesis. Eur. J. Neurosci. 24, 1935–1945.
Lahtinen, L., Huusko, N., Myohanen, H., Lehtivarjo, A.K., Pellinen, R., Turunen, M.P., Yla-Herttuala, S., Pirinen, E., Pitkanen, A., 2009. Expression of urokinase-type plasminogen activator receptor is increased during epileptogenesis in the rat hippocampus. Neuroscience 163, 316–328.
Lahtinen, L., Ndode-Ekane, X.E., Barinka, F., Akamine, Y., Esmaeili, M.H., Rantala, J., Pitkanen, A., 2010. Urokinase-type plasminogen activator regulates neurodegeneration and neurogenesis but not vascular changes in the mouse hippocampus after status epilepticus. Neurobiol. Dis. 37, 692–703.
Levitt, P., 2005. Disruption of interneuron development. Epilepsia 46 (Suppl 7), 22–28.
Liu, B., Zhang, B., Wang, T., Liang, Q.C., Jing, X.R., Zheng, J., Wang, C., Meng, Q., Wang, L., Wang, W., Guo, H., You, Y., Zhang, H., Gao, G.D., 2010. Increased expression of urokinase-type plasminogen activator receptor in the frontal cortex of patients with intractable frontal lobe epilepsy. J. Neurosci. Res. 88, 2747–2754.
Madinier, A., Quattromani, M.J., Sjolund, C., Ruscher, K., Wieloch, T., 2014. Enriched housing enhances recovery of limb placement ability and reduces aggrecan-containing perineuronal nets in the rat somatosensory cortex after experimental stroke. PLoS One 9, e93121.
Morales, D., McIntosh, T., Conte, V., Fujimoto, S., Graham, D., Grady, M.S., Stein, S.C., 2006. Impaired fibrinolysis and traumatic brain injury in mice. J. Neurotrauma 23,

976–984.
Ndode-Ekane, X.E., Pitkanen, A., 2013. Urokinase-type plasminogen activator receptor modulates epileptogenesis in mouse model of temporal lobe epilepsy. Mol. Neurobiol. 47, 914–937.
Nicolas, L.B., Kolb, Y., Prinssen, E.P., 2006. A combined marble burying-locomotor activity test in mice: a practical screening test with sensitivity to different classes of anxiolytics and antidepressants. Eur. J. Pharmacol. 547, 106–115.
Nissinen, J., Andrade, P., Natunen, T., Hiltunen, M., Malm, T., Kanninen, K., Soares, J.I., Shatillo, O., Sallinen, J., Ndode-Ekane, X.E., Pitkanen, A., 2017. Disease-modifying effect of atipamezole in a model of post-traumatic epilepsy. Epilepsy Res. 136, 18–34.
Ploug, M., Ronne, E., Behrendt, N., Jensen, A.L., Blasi, F., Dano, K., 1991. Cellular receptor for urokinase plasminogen activator. Carboxyl-terminal processing and membrane anchoring by glycosyl-phosphatidylinositol. J. Biol. Chem. 266, 1926–1933.
Powell, E.M., Campbell, D.B., Stanwood, G.D., Davis, C., Noebels, J.L., Levitt, P., 2003. Genetic disruption of cortical interneuron development causes region- and GABA cell type-specific deficits, epilepsy, and behavioral dysfunction. J. Neurosci. 23, 622–631.
Price, M.G., Yoo, J.W., Burgess, D.L., Deng, F., Hrachovy, R.A., Frost Jr, J.D., Noebels, J.L., 2009. A triplet repeat expansion genetic mouse model of infantile spasms syndrome, Arx(GCG)10+7, with interneuronopathy, spasms in infancy, persistent seizures, and adult cognitive and behavioral impairment. J. Neurosci. 29, 8752–8763.
Rantala, J., Kemppainen, S., Ndode-Ekane, X.E., Lahtinen, L., Bolkvadze, T., Gurevicius, K., Tanila, H., Pitkanen, A., 2015. Urokinase-type plasminogen activator deficiency has little effect on seizure susceptibility and acquired epilepsy phenotype but reduces spontaneous exploration in mice. Epilepsy Behav. 42, 117–128.
Sallinen, J., Holappa, J., Koivisto, A., Kuokkanen, K., Chapman, H., Lehtimaki, J., Piepponen, P., Mijatovic, J., Tanila, H., Virtanen, R., Sirvio, J., Haapalinna, A., 2013. Pharmacological characterisation of a structurally novel alpha2C-adrenoceptor antagonist ORM-10921 and its effects in neuropsychiatric models. Basic Clin. Pharmacol. Toxicol. 113, 239–249.
Sato, S., Kopitz, C., Schmalix, W.A., Muehlenweg, B., Kessler, H., Schmitt, M., Kruger, A., Magdolen, V., 2002. High-affinity urokinase-derived cyclic peptides inhibiting urokinase/urokinase receptor-interaction: effects on tumor growth and spread. FEBS Lett. 528, 212–216.
Smith, H.W., Marshall, C.J., 2010. Regulation of cell signalling by uPAR. Nat. Rev. Mol. Cell Biol. 11, 23–36.
Sorg, B.A., Berretta, S., Blacktop, J.M., Fawcett, J.W., Kitagawa, H., Kwok, J.C., Miquel, M., 2016. Casting a wide net: role of perineuronal nets in neural plasticity. J. Neurosci. 36, 11459–11468.
Wiley, C.A., Bissel, S.J., Lesniak, A., Dixon, C.E., Franks, J., Beer Stolz, D., Sun, M., Wang, G., Switzer, R., Kochanek, P.M., Murdoch, G., 2016. Ultrastructure of diaschisis lesions after traumatic brain injury. J. Neurotrauma 33, 1866–1882.
Wintergerst, E.S., Vogt Weisenhorn, D.M., Rathjen, F.G., Riederer, B.M., Lambert, S., Celio, M.R., 1996. Temporal and spatial appearance of the membrane cytoskeleton and perineuronal nets in the rat neocortex. Neurosci. Lett. 209, 173–176.